Optical Materials xxx (2008) xxx–xxx

Contents lists available at ScienceDirect

Optical Materials

journal homepage: www.elsevier.com/locate/optmat

Batch process for the fabrication of $LiNbO_3$ photonic crystals using proton exchange followed by CHF_3 reactive ion etching

G. Ulliac [a], N. Courjal [a,*], H.M.H. Chong [b,c], R.M. De La Rue [b]

[a] Department of Optics, Institut FEMTO-ST, 1- rte de Gray, UMR CNRS 6174, 25030 Besançon Cedex, France
[b] Department of Electronics and Electrical Engineering, University of Glasgow, Scotland, UK
[c] Nanoscale Systems Integration Group, School of Electronics and Computer Science, University of Southampton, Southampton SO17 1BJ, United Kingdom

ARTICLE INFO

Article history:
Received 5 December 2007
Received in revised form 27 February 2008
Accepted 11 March 2008
Available online xxxx

PACS:
42.70.a
77.84.Dy
85.40.Hp
81.65.Cf
85.40.ux

Keywords:
Lithium niobate
Reactive ion etching
Proton exchange
Batch fabrication

ABSTRACT

We report a simple process for the batch fabrication of photonic crystals in lithium niobate substrates. By means of proton-exchange (PE) followed by CHF_3 reactive ion etching (RIE) we have achieved structures with a diameter of 400 nm and an aspect ratio (depth-to-diameter) of 3:1. Sub-micrometric structures have been fabricated with an 85° angle between the walls and the plane of the substrate. We provide the optimized parameters – and their influence on the aspect ratio, the etching rate and the verticality of the walls. Transversal cross-section micrographs of the etched patterns, for both X-cut and Z-cut substrates, are shown as a clear evidence of the capability developed.

Contents

1. Introduction

Lithium niobate waveguides are used extensively in integrated optics, owing to their low optical losses and large electro-optical, nonlinear and piezoelectric coefficients. Moreover, their large range of transparency (350–5500 nm) offers the capability of covering not only the telecommunication bands, but also optical bands that are more specific to medical or aero-space applications [1].

However, the typical size of lithium niobate components (1 cm or more) represents a large handicap for their integration into dense optical circuits. A solution has been proposed recently, based on photonic crystal (PhC) structures that replace the traditional Mach–Zehnder interferometer. Roussey et al. [2] have shown that the active length of the modulators in lithium niobate may thereby be reduced to as little as 13 μm. These results open the way to compact high-bandwidth intensity modulators that could compete with electro-absorption modulators in terms of extinction ratio and operating wavelength range. There are numerous papers dedicated to theoretical and experimental studies of $LiNbO_3$ PhCs,

* Corresponding author. Tel.: +33 3 81 85 39 34; fax: +33 3 81 66 64 23.
E-mail address: nadege.bodin@univ-fcomte.fr (N. Courjal).

0925-3467/$ - see front matter © 2008 Elsevier B.V. All rights reserved.
doi:10.1016/j.optmat.2008.03.004

showing that $LiNbO_3$ intensity modulators are not the only outlet for $LiNbO_3$ PhCs. For example, the use of 1D PCs has been reported [3] for the fabrication of an integrated squeezing circuit. Moreover, theoretical work has shown the considerable potential for further development of $LiNbO_3$ PhCs [4,5].

The main method that has been reported until now for the fabrication of $LiNbO_3$ PhCs is based on focused ion beam (FIB) milling [6,7]. This method has been shown to be very effective for the fabrication of small area structures (e.g. arrays of less than 50×50 holes). But FIB milling is performed on a hole-by-hole basis, which implies long process times and eventual drift when fabricating large fields of photonic structures. An alternative approach consists of ferroelectric domain inversion, followed by wet etching [8]. The method is limited to Z-cut substrates. Ultrafast laser machining is a robust technique amenable to patterning any material. A recent paper has shown the feasibility of the technique for the fabrication of polaritonic structures in $LiNbO_3$ substrates [9]. The advantage is that it allows the production of trenches as deep as several hundred micrometers. But the application of this method to photonic structures would require the laser spot to be focused to or near the diffraction limits. The feature sizes achievable by laser machining are currently not small enough for the patterning of photonic crystal structures that operate at near-infrared or visible wavelengths. Common alternatives include preparing the etching of the substrate by modifying the crystal lattice. Ion implantation or proton exchange (PE) are well known approaches for producing such alteration [10–14]. Amongst the methods reported, the combination of PE with plasma etching is the most attractive in terms of cost, reproducibility and control of under-etching. In Ref. [14], this combination was applied to the fabrication of PhC structures. The etching process reported in Ref. [14] used ICP–RIE (inductively coupled plasma) etching applied to the processing of Z-cut substrates.

Here, we describe a process based on RIE etching that allows the fabrication of PhCs with an aspect ratio of 3, without the requirement for ICP. The fabrication process is detailed with cross-sectional views of the patterns produced. The process applies for both X-cut and Z-cut structures.

2. Description of the process

The process is depicted schematically in Fig. 1. Firstly, a 250 nm thick layer of poly-silicon is sputtered onto the substrate. A positive resist is then spin-coated onto the substrate – and patterned by either direct write electronic-beam lithography (EBL) or deep ultra-violet (DUV) lithography. The electron-beam resist used in this work is ZEP520A and the pattern is written using an accelerated beam voltage of 100 kV. The pattern is then transferred to the mask layer by means of RIE based on SF_6 chemistry.

Proton exchange (PE) is performed through the silicon mask layer in a bath of molten benzoic acid. The temperature of the bath is chosen to be rather low (typically 190 °C), in order to produce a significant lattice deformation [1], which will facilitate further etching. The duration of the PE steps depends on the substrate chosen. Typically, an exchange-depth of 1.5 μm corresponds to 6.5 h duration of proton exchange on X-cut substrates [16], and 12.6 h duration of proton exchange on Z-cut substrates [17]. The replacement of Li^+ ions with H^+ protons helps to prevent LiF re-deposition during the RIE step, which plays a role in both the verticality of the structures and the etch-rate [13].

In a third step, the pattern is written into the substrate by CHF_3 RIE etching. The etching is carried out using a Plassys reactor with a maximum power of 300 W. The aim is to make the plasma react preferentially with the proton-exchanged areas, while leaving non-exchanged areas intact. In order to enhance the chemical aspect of the RIE etching, we have worked with CHF_3 gas at relatively high pressures (more than 25 μbar), and RF power levels lower than 200 W. The parameters are detailed in Fig. 1: the RF power and the operating pressure were tested on a range of 50–200 W and 25–100 μbar, respectively. The poly-silicon mask layer was chosen because of its resistance to PE and its enhanced selectivity during the CHF_3 RIE etching step. Indeed, the CHF_3 plasma is composed of CF_X radicals that react with F atoms and create a C_XF_Y insulating polymer deposit on the surface of the silicon layer [15]. The creation of an additive protective layer was confirmed by testing with a CHF_3/O_2 reactive plasma. After 1 h of RIE processing, the silicon mask layer was totally etched away, due to the reaction of C_xF_Y with O_2. The same test performed without O_2 gas left the mask intact.

Finally, the remaining silicon mask layer is etched away using a SF_6 plasma.

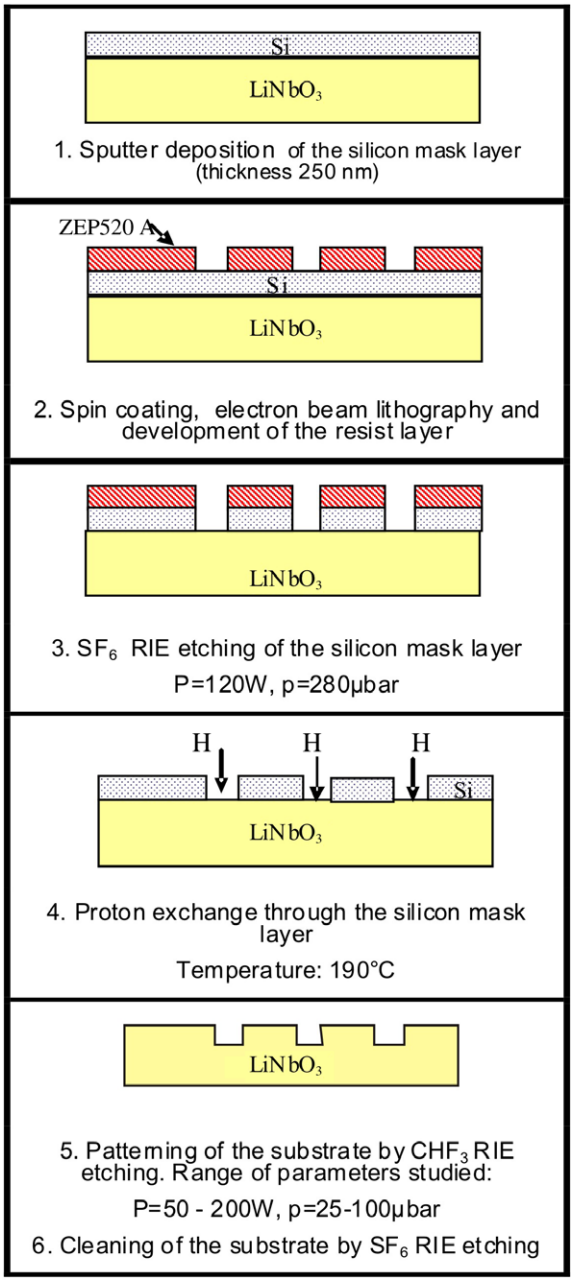

Fig. 1. Fabrication process steps and associated parameters.

Please cite this article in press as: G. Ulliac et al., Opt. Mater. (2008), doi:10.1016/j.optmat.2008.03.004

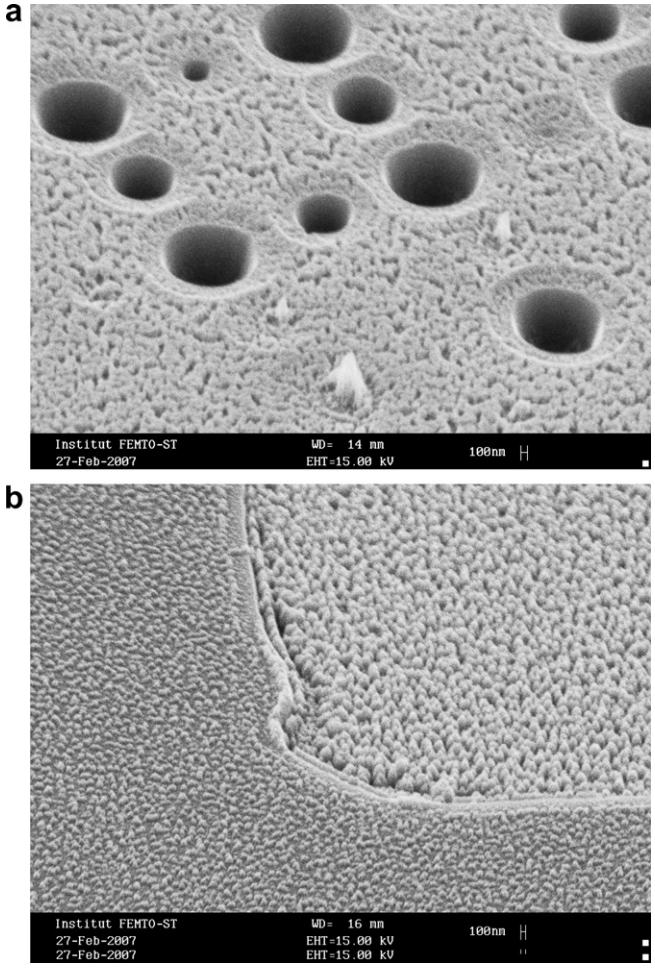

Fig. 2. SEM images of patterns written in a $LiNbO_3$ X-cut substrate. The diameters of the test patterns vary from 200 nm to 1 μm. The operating gas is CHF_3, the RF power level is of 150 W, and the gas pressure is 100 μbar. (a) With a previous PE step. (b) Without a previous PE step.

3. Experimental results and discussion

The influence of the PE step is illustrated in Fig. 2. The same RIE conditions were used for both Fig. 2a and b with an RF power level of 150 W, an operating pressure of 100 μbar and CHF_3 as operating gas. The substrate surface remains un-etched where it has not previously been prepared using PE (Fig. 2b), whereas it is etched to a depth of 1.5 μm where it has previously been proton-exchanged (Fig. 2a). The maximum etching rate of the untreated material is estimated to be 110 nm/h, which is 6.5 times slower than the etch-rate of the treated material. Moreover, the patterns of the untreated material appear to be very rough, which may be due to the re-deposition of LiF during the etching process.

As previously mentioned, the substrate cannot be etched in zones where the proton-exchange process has not occurred. But an inappropriately long duration of PE may also lead to significant spreading of the exchange process under the mask – which will cause under-etching during the RIE step. This under-etching becomes obvious when the exchanged layer is deeper than 2.5 μm. The optimum exchange-depth has been determined to be 1.5 μm.

The influence of the operating RF power and the gas pressure on the etching behaviour is shown in Fig. 3 for holes with a surface of 10 μm × 10 μm. Step heights were measured with a Tencor Alpha-step profilometer.The etching rate becomes progressively larger as the power increases and the pressure decreases. We have nevertheless noticed that a high power level (>200 W) tends to produce a deterioration in the quality of the substrate surface. It should also be emphasized that the selectivity of the mask diminishes when the pressure is below 30 μbar or the RF power is above 150 W. Thus, a compromise between surface quality, selectivity and etching rate can be reached by choosing a 100–150 W RF power level, and a pressure of 40–60 μbar. Typically, the etching rate with such parameters varies from 6 nm/min to 12 nm/min (see Table 1). The results given in Table 1 also show that the etch-rate of $LiNbO_3$ is linked to the dimension of the holes: for the same RIE conditions, the etch-rate is lowered by a factor of two when the size of the hole decreases from 2 μm to 1 μm. Thus, the fabrication of PhCs will take more time for a given area of structuring than the fabrication of standard, larger feature size, micrometric structures.

In Table 1, we show the measured angles and depths of submicrometric structures obtained from FIB process cross-sectional images. According to these results, the angle between the axes of the holes and the plane of the substrate is weakly dependent on the size of the holes, properties that are characteristic of this process. Indeed, other tests performed with higher RF power levels (200 W), low operating pressure (3 μbar), and SF_6 gas indicate that, when the sputtering process is enhanced during RIE, the angle of the sidewall decreases with the size of the hole, i.e. the sidewalls of the holes are less steep.

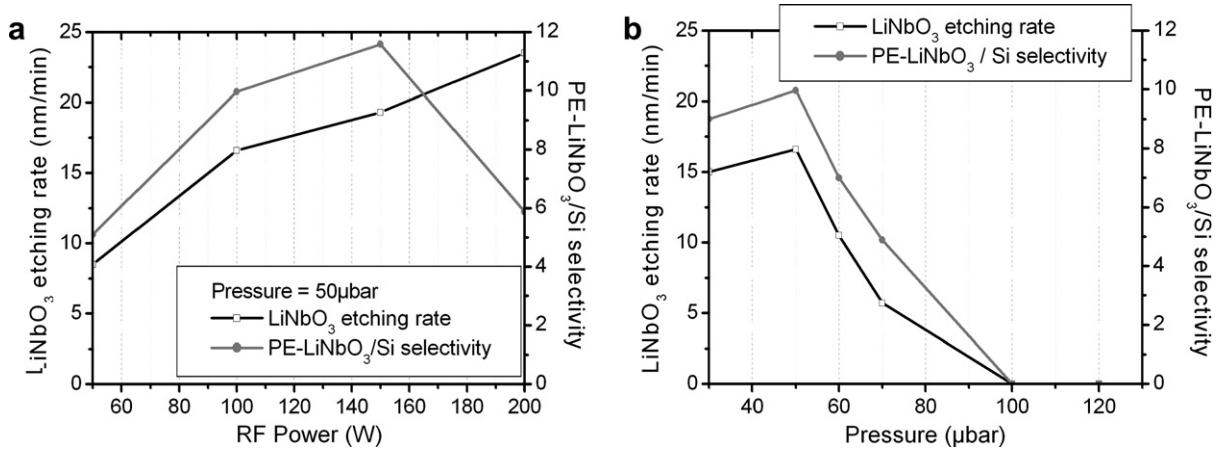

Fig. 3. The figure shows (a) the influence of the power level on the etching process on X-cut substrates, for an operating pressure of 50 μbar. (b) The influence of the operating pressure on the etching process in X-cut substrates, for an RF power level of 100 W. The measurements were performed on holes with a surface of 10 μm × 10 μm.

Table 1
Evaluation of the characteristics of the etched holes in a X-cut substrate

Pressure (μbar)	RF power (W)	Time (min)	Depth of the holes (μm)	Diameter of the holes (μm)	Angle (°)	Aspect ratio	V_{LiNbO_3} (nm/mn)	Selectivity $LiNbO_3$/Si
60	100	140	1.2	0.4	85	3	8.5	4.7
70	100	210	1.27	1.6	58	0.8	6.0	5.0
80	150	175	0.98	1	63	1.0	5.6	2.8
80	150	175	1.36	1.3	64	1.0	7.7	3.9
80	150	175	1.93	2	63	1.0	11.0	5.5
100	150	140	1.63	1.8	61	0.9	11.6	4.6

In Figs. 4 and 5, we show SEM images of patterns (pillars or holes) achieved with optimized pressure and power levels. The influence of gas pressure on the aspect ratio of the structure was evaluated from the SEM images. In Fig. 4a, the pillars were processed at a pressure level of 60 μbar, whereas the operating pressure was 100 μbar for the structure shown in Fig. 4b. These images illustrate the increase of the structure verticality with decreasing pressure: the etched structures exhibit an improvement of 8° in their verticality when the pressure is reduced from 100 μbar to 60 μbar. Below 60 μbar, the angle is no longer influenced by pressure. Fig. 4b and c shows that the RF power level influences the smoothness of the patterns. The walls of the pillars become progressively smoother as the power level is lowered.

Holes with a diameter of 420 nm, a depth of 1.2 μm and a sidewall-angle of 85° are shown in Fig. 5, resulting from the optimisation of the RIE process parameters. Such parameters meet the requirements for practical $LiNbO_3$ PhC structure fabrication [1]. Fig. 6 shows an SEM image of a large field $LiNbO_3$ PhC structure produced using these conditions. It should be noted that, apart from the duration of the PE exchange, the same process was used for both X-cut and Z-cut substrates, and no significant difference was noted between the results obtained on the two kinds of substrates. The above results can be compared with those achieved by FIB milling in Ref. [6]. The roughness that can be seen on the transversal view is similar to that seen on structures patterned by FIB. We are currently working on the implementation of such PhC structures in PE waveguide layers. Though the optical characterization has not yet been performed, we can infer from preliminary work [2] that the results reported in this paper could enable the fabrication of 2D photonic bandgap structures.

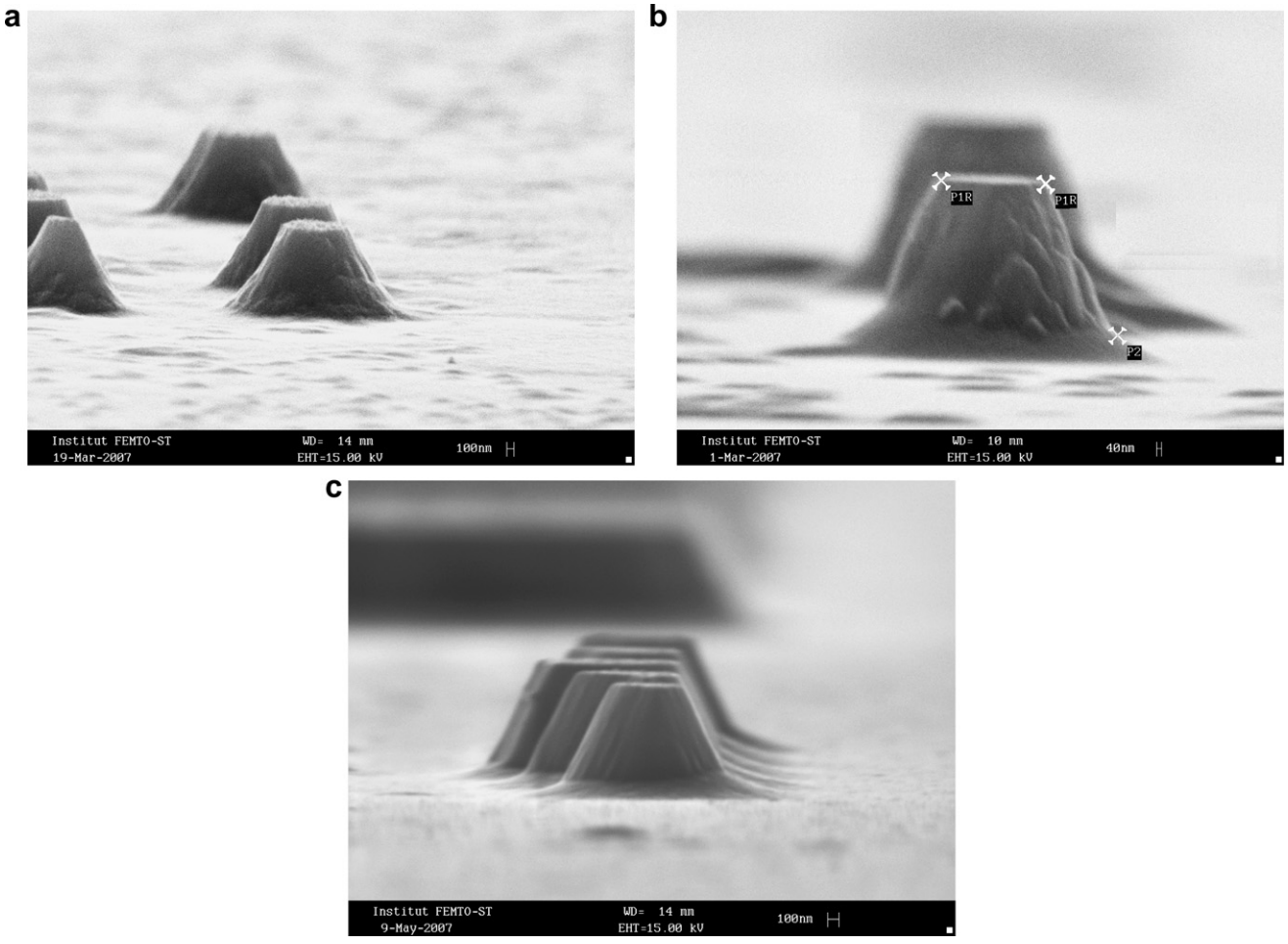

Fig. 4. SEM images of Z-cut substrates after etching of the Si mask layer. (a) The gas pressure is p = 100 μbar and the RF power is P = 150 W. After 180 min of RIE the resulting angle is measured to be 56°. (b) The gas pressure is p = 60 μbar and the RF power level is P = 150 W. After 135 min of RIE the resulting angle is measured to be 64°. (c) The gas pressure is p = 60 μbar and the RF power is P = 100 W. After 300 min of RIE the resulting angle is measured to be 64°.

Please cite this article in press as: G. Ulliac et al., Opt. Mater. (2008), doi:10.1016/j.optmat.2008.03.004

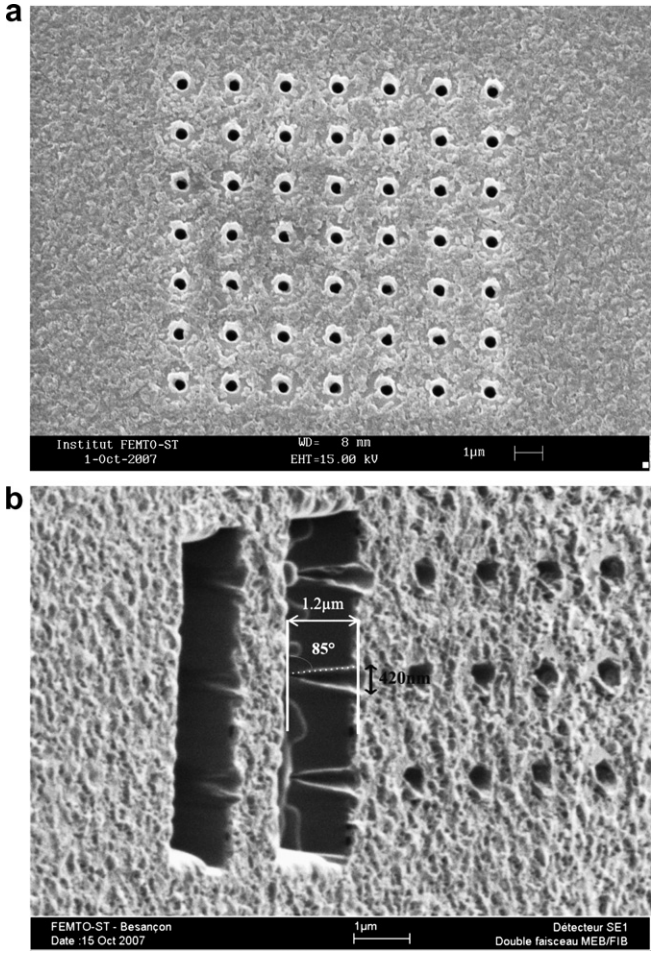

Fig. 5. SEM images of an X-cut substrate after etching of the Si mask layer. The gas pressure is $p = 60$ μbar, the RF Power is $P = 100$ W. The images are obtained after 140 min of RIE etching. The resulting depth is measured to be 1.2 μm. (a) Overall view. (b) Transversal section of the holes realised by FIB milling

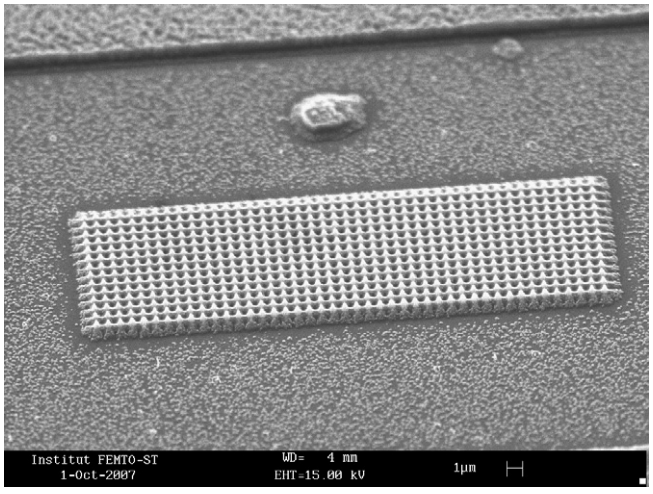

Fig. 6. SEM image of a 45 × 15 periodic square array of holes, with period = 766 nm and diameter = 400 nm. The gas pressure is 60 μbar and the RF power is 100 W. The images are obtained after 100 min of RIE etching.

4. Conclusions

We have shown the possibility of fabricating large fields of photonic crystal structure on lithium niobate substrates. The method typically starts with electron-beam lithography. With this approach, fields of photonic crystal structure with areas on the order of a few square millimetres may be obtained. Subsequent process steps are based on proton-exchange and CHF_3-based RIE. The parameters of the RIE process were optimized – and it was found that an RF power level of 100–150 W and an operating pressure of 40–60 μbar could produce sub-micrometric structures with an aspect ratio of 3:1. The cross-sectional micrographs of the patterns show angles of 85° between the surface of the substrate and the side-walls of the holes. The method opens the way for the production of densely integrated $LiNbO_3$ PhC-based devices over large areas.

Acknowledgments

This work was supported by the Action Concertée Incitative "Nanosciences" COBIAN, No. NR137. The authors wish to acknowledge Blandine Guichardaz, Denis Bitschene, Jean-Yves Rauch and Roland Salut for technical assistance. Partial support through the ePIXnet European Network of Excellence is also acknowledged.

References

[1] L. Lawrence, Rep. Prog. Phys. 56 (1993) 363.
[2] M. Roussey, M.-P. Bernal, N. Courjal, F.I. Baida, R. Salut, Appl. Phys. Lett. 89 (2006) 241110.
[3] G.S. Kanter, P. Kular, R. Roussev, K.R. Parameswaran, M.M. Fejer, Opt. Exp. 10 (2002) 177.
[4] K.C. Huang, P. Bienstman, J.D. Joannopoulos, K.A. Nelson, S. Fan, Phys. Rev. Lett. 90 (2003) 196402.
[5] M. Roussey, F.I. Baida, M.P. Bernal, JOSA B 24 (2007) 1416.
[6] F. Lacour, N. Courjal, M.P. Bernal, M. Spajer, A. Sabac, C. Bainier, Opt. Mater. 27 (2005) 1421.
[7] S. Yin, Proc. IEEE 87 (1999) 1962.
[8] I.E. Barry, G.W. Ross, P.G.R. Smith, R.W. Eason, G. Cook, Mater. Lett. 37 (1998) 246.
[9] D.W. Ward, E.R. Startz, K.A. Nelson, Appl. Phys. A, Mater. Sci. Proc. 86 (2007) 49.
[10] K. Mizuuchi, K. Yamamoto, T. Taniuchi, Electron. Lett. 26 (1990) 1992.
[11] F. Laurell, Jonas Webjörn, G. Arvidsson, J. Holmberg, J. Lightwave Technol. 10 (1992) 1606.
[12] T.-J. Wang, C.-F. Huang, W.S. Wang, P.-K. Wei, J. Lightwave Technol. 22 (2004) 1764.
[13] D.M. Gill, D. Jacobson, C.A. White, D.W. Jones, Y. Shi, W.J. Minford, A. Harris, J. Lightwave Technol. 22 (2004) 887.
[14] H. Hu, A.P. Milenin, R.B. Wehrspohn, H. Hermann, W. Sohler, J. Vac. Sci. A 24 (A) (2006) 1012.
[15] J. Penaud, Thesis, University of Lille, 2006.
[16] T. Maciak, M. Solowski, Opt. Appl. 29 (1989) 423.
[17] D.F. Clark, A.C.G. Nutt, K.K. Wong, P.J.R. Laybourn, R.M. De La Rue, Appl. Phys. Lett. 54 (1983) 6218.